Bacteria accumulate copper ions and inhibit oxide formation on copper surface during antibacterial efficiency test

Jiaqi Luo, Christina Hein, Jaafar Ghanbaja, Jean-François Pierson, Frank Mücklich

Version of Record: https://www.sciencedirect.com/science/article/pii/S0968432819302628
Manuscript_3cadd3237936d500144fe5199a6da994

Bacteria accumulate copper ions and inhibit oxide formation on copper surface during antibacterial efficiency test

Jiaqi Luo[a,b,*], Christina Hein[c], Jaafar Ghanbaja[b], Jean-François Pierson[b], Frank Mücklich[a]

[a] Functional Materials, Saarland University, Germany

[b] Université de Lorraine, CNRS, IJL, F-54000 Nancy, France

[c] Inorganic Solid State Chemistry, Saarland University, Germany

[*] Email address: jiaqi.luo@uni-saarland.de

Abstract

Copper surface after antibacterial test against *E. coli* was examined in the aspect of corrosion. Results from scanning electron microscope (SEM), grazing incidence X-ray diffractometer (GIXRD) and Raman spectroscopy together confirmed less oxidation on copper surface with the presence of *E. coli*. The inhibition of the cuprous oxide (Cu_2O) layer instead ensured the continuous exposure of copper surface, letting localised corrosion attacks observable and causing a stronger release of copper ions. These phenomena are attributed to the fact that *E. coli* act as ions reservoirs where high amount of copper accumulation were found by energy dispersive X-ray spectroscopy (EDS).

Keywords: copper, oxidation, ions, ICP-MS, EDS, *E. coli*

1. Introduction

Copper has been drawing the attention of microbiologists in the recent years [1-4]. Copper and its ions, copper oxides as well as oxide nanoparticle, all of them have shown the toxicity against various bacteria or virus [5, 6]. This antimicrobial property brings copper into the hygiene market, and without a doubt, a great amount of studies have focused on this aspect. Copper or copper contained coatings [7, 8], particles [9, 10], fabrics [11, 12], textiles [13, 14], composites [15, 16] are being fabricated and widely investigated, in terms of their antimicrobial efficiencies the relevant applications.

To determine the antimicrobial efficiency of a certain material, or more specifically of a surface, a certain method has to be applied. It allows us to measure the survival of microbe, to quantify the antibacterial efficacy, and in the end, to compare them. Most of these methods could be grouped into two main types that worth being briefly introduced. One is where no suspension with bacteria needs to be prepared, for instance, in the inhibition zone determination [15, 17]. The coupon to be tested will be placed on a nutrient agar plate already covered with bacteria. Since the antibacterial agents could release and further diffuse from the coupon, a gradient of antibacterial substance is supposed to form from the centre of the coupon outwards. After certain incubation periods, there should be a zone around the coupon where no obvious growth of colony is observed. The antibacterial efficiency can be thus compared by the size or radius of these zones. Moreover, this method may tell better the diffusion rate of the corresponding antibacterial substance on the agar plate. It is fairly popular in research especially in testing novel antibacterial composites or fabrics.

In another type of method, a drop of suspension composed of bacteria and buffer solution needs to be applied on the coupon. After several designed time points, part of the suspension is withdrawn. There are a number of approach to determine the bacterial survival in the suspension. One way to do this is by fluorescence microscopy [18, 19], which is also often called Live/Dead staining test. In this test, a red-fluorescent indicator (often propidium iodide) is used to label the DNA after membrane damage happens, so as to distinguish whether bacteria are intact or not. Therefore the change of colour directly tells the killing effect of a substance. Another popular approach is to count the colony-forming unit (CFU) [20, 21]. The withdrawn suspension will be first properly diluted in series and then plated on an agar plate. The cultivable bacteria will grow as colonies that could be big enough to be identified and directly counted. This method not only produces highly statistical and reproducible results, but also allows to track the details of antibacterial efficiency as a function of time. This is why it has been chosen in most of our recent studies [22-24], and again applied in this study.

Although all the methods listed above offer almost sufficient information of the survival of bacteria, nevertheless, there is a hidden respect not being considered: the coupons themselves. The bacteria are inactivated by the antibacterial agents, which are released from the specific surface in most of the cases. This indicates that the surface itself is also under a series of change along the time. In the case of copper, it is corrosion that should be further considered [25, 26]. Furthermore, the corrosion phenomena occurring on the surface, in fact, also alter the surface itself during these antibacterial efficiency tests.

In other words, these methods are not always charactering the initial surface, in contrary, a constantly changing surface. Take this into account have two main advantages: one is to know exactly the actual surface being characterised, the other one is to start exploring its potential aging effects when it comes to the daily life applications.

Oxidation is certainly drawing attention among the common corrosion phenomena. By mainly electrochemical means, copper oxides growth on copper or its alloys in buffer solution [27] or synthetic perspiration [28] are recently reported. Different types of oxides (Cu_2O, CuO), hydroxide ($Cu(OH)_2$) or other corrosion products ($Cu_2Cl(OH)_3$) could be identified. Their thickness and in-depth distribution were correlated with different experimental conditions, such as the chemical composition of the original surface, the components of the applied solution and the contact period. However, there is a few research that has considered the aging of copper surface in a bacterial suspension, not to mention to probe the role of bacteria in this corrosion system. On the other hand, how bacteria interact with or influence by various kinds of metallic ions or particles have been extensively investigated, in terms of the transportation of ions and the accumulation in different organelles [29, 30]. But again, bacterial influence on the surface through these effects are not the focus in these studies.

One recent research [31] revealed the re-release of silver from the silver-killed bacteria back to the solution. It offers a hint about the interaction between ions enriched bacteria and their effect on the environment. Here in the current study, we extended the focus from the solution back to the initial ions releaser: the copper surface itself. The main question we aim to answer is: during the copper release process that kills bacteria, does the existence of these bacteria affect the corrosion process as well? Therefore we investigated the role of *E. coli* in copper surface chemical changes during the antibacterial efficiency test. Ex-situ approaches were performed to distinguish the changes in morphology and composition in the outermost copper surface. The inhibition effect of oxides was described and its possible causes were put forward, taking account of the role of bacteria on the amount of copper ion in suspension.

2. Materials and Methods

2.1. Materials

Coupons of copper (99.99%, K09, Wieland) were first ground with a silicon carbide sandpaper (end with grit number as P600), then they were cleaned by an ultrasonic bath with ethanol and finally dried by air.

2.2. Solutions

Phosphate-buffered saline (PBS) was prepared with NaH_2PO_4. $1H_2O$ (Merck, Germany, final concentration 0.01 M), NaCl (VWR, Germany, final concentration 0.14 M) and pure water for analysis (Merck, Germany). Its pH value was adjusted by adding NaOH to 7.4, sterilised by an autoclave after preparation. The preparation of PBS with bacteria could also be referred to the antibacterial efficiency determination in previous publication [32]. In brief, the *E. coli* K12 strain was grown aerobically overnight in Lysogeny broth (LB) medium at 37 ºC in a water bath with a speed of 220 rpm. The stationary cells from 5 mL

culture were collected by centrifugation for 15 min at 5000 x g, washed and centrifuged three times with PBS, and finally re-suspended in 5 mL of the same type of buffer solution. The initial average cell count was around 3 X 10^9 to 5 X 10^9 CFU/ml. For the suspension *S. cohnii*, the Tryptic soy broth (Fluka) medium was chosen.

2.3. Corrosion protocol

Coupons of copper were placed in a water-saturated atmosphere at room temperature when 20 µL of various solutions were applied on them with a pipette. After certain exposure time (30 minutes, 1 hours, 3 hours and 6 hours), these solutions were withdrawn with a pipette and the coupons were dried in a ventilated room. These steps are chosen in order to keep it as similar as the antibacterial efficiency tests as described in our other research [22, 24].

2.4. Surface corrosion characterization

Scanning electron microscope (SEM, Helios NanoLab600, FEI) was used to compare the morphology of copper surfaces after various corrosion experiments. The chemical composition was obtained by Energy dispersive X-ray spectroscopy (EDS) with an acceleration voltage as 5 kV. For further confirmation of corrosion products covering the surfaces as well as the form of copper in bacteria, Raman spectroscopy (Raman, laser source with 633 nm, inVia, Renishaw) with a 50X optical microscopy (OM) and high resolution grazing incidence X-ray diffractometer (GIXRD, Cu Kα with 1 degree grazing angle, PANalytical X'Pert PRO-MPD) were applied. All these images and spectra were obtained within 24 hours after corrosion treatment.

2.5. pH values measurements

The pH values were obtained from pH-indicator strips (Merck, Germany), designed for a range from 6.5 to 10.0, with 5 gradations between 7.1 and 8.1, namely 7.1, 7.4, 7.7, 7.9 and 8.1. During the withdrawal process described in section 2.3, 10 µL of various solutions were separated and applied again on these strips.

2.6. Copper content determination

For the samples (PBS or PBS with *E. coli*) to be directly measured, following almost every step in the corrosion protocol, only whenever the exposure time is reached, 10 µL samples were withdrawn by repetitive pipetting and diluted in 2.990 mL 1 wt% nitric acid (Merck, Germany). For the measurement of supernatant, every three 10 µL samples were transferred and mixed in SafeSeal 1.5 mL tubes. After being centrifuged for 5 min at 5 krpm, 10 µL of supernatant were collected and diluted in nitric acid as mentioned above. For all samples, before measured by inductively coupled plasma mass spectrometry (ICP-MS, 7500cx, Agilent), 3 µl of 10 mg/l scandium and caesium internal standard solutions were added to the samples. For calibration, standards with 0.1, 0.5, 2.5, 10, 50, 250 and 1000 µg/L of copper were used. After obtaining the results with a unit of ppb, the final values with a unit of µM were calculated with the fold of dilutions and molar mass 63.55 g/mol for copper. The average values and standard deviation were obtained by three independent experiments.

2.7. Bacteria imaging and chemical mapping

Scanning transmission electron microscopy (STEM) mode of transmission electron microscopy (TEM, JEM-ARM 200F, JEOL) was applied with a voltage of 200 kV. The bacteria were treated with copper surface for 3 hours as described above.

Before having them transferred on a Ni grid, they were diluted 1:10 with pure water for analysis.

3. Results and Discussion

Evolution of surface morphology always reflects the corrosion behaviours. Therefore, to directly observe the corrosion phenomena on copper surface, high resolution SEM images were taken and shown in Figure 1. After 3 hours in pure PBS, granular sub-micron formation were found on the copper surface. Consequently, the as-ground morphology becomes less obvious. However, with the addition of *E. coli*, similar corrosion products can hardly be found. In addition to the remained bacteria, some area were suffering localised corrosion attacks, resulting in sub-micron scale pits. No other SEM observable features that can be identified on this bacterial treated surface. On the other side, it almost kept the original morphology of the untreated as-ground copper surface (SI, Figure 1).

To further identify these corrosion products, GIXRD were applied to collect the near surface phase information presented in Figure 2 (a). The range of diffraction peak of (111) planes of Cu_2O was chosen, since it is expected to be the strongest peak of the Cu_2O without any preferential orientation growth. A clear peak is recorded from the surface corroded by pure PBS, confirming the main corrosion products described above as crystallised Cu_2O. By contrast, the diffractogram from the coupon treated with *E. coli* suspension is rather flat.

Since no copper oxides related diffraction peaks could be assigned, Raman was applied owing to its higher sensitivity, where a slight oxidation is shown (Figure 2 (b)). Comparatively, these oxides signals are with lower background and less obvious oxides' peaks, especially around 149 cm^{-1} and 216 cm^{-1}. In addition, compared to the relatively large detection zone of GIXRD, Raman results could be correlated with more localised features. For example in Figure 2 (c), some dark areas found in OM are confirmed by SEM as the positions where localised corrosion attacks occurred. In these positions, higher Raman signal of Cu_2O were recorded and shown in Figure 2 (d). Although these localised corrosion sites are far smaller than the macroscopic pits that could be observed directly in OM, they do match the features described traditional pitting corrosion theories [33]. They describe the formation of corrosion products around the opening (cathode) of these cavities (anode). These product could gradually seal the pits, which has not yet been observed on our experiments though. Apart from small difference, all the abovementioned findings confirm the considerable changes on copper surface after adding *E. coli* into PBS: the Cu_2O formation becomes less dominant and more non-uniform on copper surface.

Corrosion behaviour of a certain material is never an independent phenomenon: it is closely correlated to the surrounding environment which is applied, that is to say, the solutions (PBS or bacterial suspensions) on copper coupons. It is known from the Poubaix diagram of copper, that Cu_2O formation favours alkaline environment, while acidity increases, it dissolves and exists as cupric ions [27]. For this reason, although PBS is defined and prepared as a buffer solution, it would still be helpful to know whether the actual condition in these corrosion tests already exceeds the buffer capacity. Therefore, the pH values of

147 the samples were checked and given in Table 1. For the original PBS, no matter with or without bacterial addition, their pH
148 values were 7.4 as designed. However, in both cases, this value rose after corrosion tests, indicating an alkaline shift. Most
149 importantly, when *E. coli* was added, the solution became even more alkaline, which theoretically should be more beneficial
150 to the formation of Cu_2O. Therefore, there must be other reasons instead of the acidity that inhibit the oxide growth in bacterial
151 condition.

152 To preliminarily verify if *E. coli* could interactive with Cu_2O actively, another case was designed to place *E. coli* PBS
153 suspension on pure PBS treated copper surface (therefore with existing Cu_2O). Their GIXRD results (SI, Figure 2) show that
154 the previously formed Cu_2O layer does not change obviously after bacterial suspension treatment, suggesting that *E. coli* do
155 not act as an active role in deteriorating Cu_2O layer.

156 After the examination of the corrosion products on these surfaces, we then shifted the interest to the solution, namely the
157 withdrawn droplets. Copper content in pure PBS and *E. coli* PBS suspension were measured and plotted in Figure 3. In pure
158 PBS, the concentration of copper has quickly reached a plateau in 30 minutes, which at least lasted for 3 hours. With *E. coli*
159 addition, on the other hand, the curve evidently follows another trend: it significantly becomes higher in the whole period.
160 The variety of these two patterns could be ascribed to the barrier effect of copper oxides coverage. As fewer oxides were
161 found in the latter case, a bigger portion of bare copper was exposed to the solution, that is to say, can still be corroded by the
162 solution. For this reason, release of copper ion can be thus less hindered and therefore copper content gradually increase could
163 be observed. In addition, the shown copper content data can also be transferred into weight loss of the original surface if
164 needed. Because for pure copper coupons, the amount of copper measured in solution should be equal to the weight loss.
165 However, it should be noted that the contribution from the oxide growth will not be considered in this way as they are still
166 attached to the original surface.

167 But why did the oxide growth rate slowdown so distinctly? Similar trends of copper content were also reported with *S.*
168 *cohnii* addition [34]. *S. cohnii* is a type of bacteria with less mobility, as shown in SI Figure 3, its PBS suspension has rather
169 similar corrosive influence on the copper surface: no obvious oxide layer could be found in 3 hours. This helps us to exclude
170 the potential effects induced by bacterial mobility that may change the local near-surface circumstance, such as substance
171 concentration and fluid flow rate.

172 Now back to the rise of copper content, which was previously ascribed to the bonding effect of complexing agents [34].
173 Inspired by this aspect, another test was designed to detect the amount of copper in supernatant (green curve in Figure 3).
174 This result implies another possibility. These values represent the amount of free copper ions in the suspension. They are
175 relatively low, fewer than those in PBS by almost a factor around 5, in spite of the slight increase along the time. It could
176 probably mean that the concentration of free copper ions are still far away from its equilibrium that leads to oxides formation.

177 Apparently, the following question needs to be answer could be: where are the rest of the huge amount of copper?
178 Logically, if they are not in the supernatant, then they could only be with bacteria. Figure 4 presents the copper treated *E. coli*

observed by SEM. Prolonging the treatment time, in the first place, the shape of bacteria becomes more regular. However, since no fixation or drying steps were adopted in order to preserve the potential copper ion accumulation within bacteria, morphology of these bacteria might not be interpreted as their original state.

On the other hand, local elemental analysis done by EDS further provides more interesting information. First of all, the main elemental composition of *E. coli* itself is always considered as a combination of C, H, O and N [35]. Other elements should be thus considered to have an environmental source. Therefore, the actual EDS on untreated *E. coli* (shown in SI Figure 4) also revealed certain amounts of Na and P, which could come from the compositions of LB growth medium or PBS. Besides, signal of Si comes from the silicon substrate that is supporting the bacteria. The most significant finding belongs to those Cu peaks. Not only have their signal been successfully collected, their intensity also progressively increases proportional to treatment time. This trend indeed represents the copper amount accumulated by the bacteria, confirming both our results and the latest reported results obtained from ICP-MS measurements [36].

As generally reported, 3-hour is a period already assures at least 99.9% *E. coli* in PBS can be killed on copper surface due to the released copper ions [24]. Interestingly, this accumulation process still continued after 3 hours, as the intensity from Cu peak reached another higher value in 6 hours. A similar test with sterile *E. coli* instead of viable *E. coli* was carried out, where bacteria were found with high copper content as well (shown in SI Figure 5). This may indicate the observed accumulation process should not be considered as an active process fulfilled by the living bacteria or biofilm, but rather a passive process in this condition. Meanwhile, these results also suggest that the inhibition of oxides are not likely to be linked with the consequences of bacterial metabolism such as the consumption of oxygen.

Apart from this type of copper accumulation, the dissolved copper exists as another observable form. Figure 5 reveals this on those bacteria after treated with copper surface for 3 hours: there are some sub-micron particles with various sizes attaching on these bacteria. EDS spectra collected from these features tell more details from their composition. Position 1 represents the spectrum obtained from bacterium without particle coverage, acting as a contrast. The present elements resemble those discussed in the above section. The intensity of Cu is relatively higher, resulting from the fact that during this observation, these bacteria were still on copper surface, instead of having been transferred to silicon wafer in the previous case. Therefore this intensity also includes the characteristic X-ray excited from the copper surface under the bacterium due to its small size (more precisely, the thickness) of bacterium. On the other hand, the spectrum from position 2 centred on the sub-micron particle draws a different scene. The intensity of C, N and Na became less, based on the fact that the particle locates higher than the bacterium, and so there was less electrons reaching and exciting characteristic X-ray from the bacterium. Whereas the other three detected elements, namely O, Cu and P, were recorded with higher intensity. They should thus be considered as the main elemental composition of these particles.

Although no exact phase composition of these particles could be indexed from the current GIXRD results, studies [37, 38] did have shown that a popular approach to produce copper phosphate nano-particle is by appropriately mixing copper or

its ions with phosphate solution. Unfortunately, we cannot directly conclude whether the bacteria promote the formation of the suspected copper phosphate particles (not the scope of our current study either). Nevertheless, we could still comment that they are more likely to grow on bacteria, and it does show us one of the forms how the copper content being stabilised in the solution instead of being free ions. Furthermore, since the above ICP-MS results only could show the sum of both accumulation of copper in bacteria and copper phosphate, it will be meaningful if future experiments are designed to show the proportion.

These sub-micron particles are easily found, mainly because their distribution on the surface of bacteria. However, for the dispersed copper that could only be detected by EDS, it is still yet to know whether they entered the bacteria or only attached with the outer membrane. STEM mode in TEM was therefore applied so as to collect the information of the elemental distribution, as shown in Figure 6. BF image outlines the profile of bacteria better. While in the ADF image, it could already be observed that the sub-micron particles contain elements with higher atomic number, since higher intensity from these locations were recorded. This information is further confirmed by EDS mapping, where O, Cu and P were found highly concentrated in those regions. Another important fact could be extracted from the EDS mapping, is the distribution of copper in a bacterium. It is true that for a 2D top-view of a 3D object (the bacterium), it's hard to tell where the copper exactly are. However, one could still suppose that if the situation was that the copper only anchored on the outer membrane of a bacterium. In this case, the copper amount should be found a significant increase from the centre of the bacterium to its edge. This is because from a 2D top-view, the edge of a bacterium consists of overlap of the membrane in top-view that should have resulted in a higher copper content. But this has not been observed in the current result, suggesting that it is highly possible that those dispersed copper were located within the bacteria. To further investigate the more precise locations of copper, further work could be done by combing other more localised techniques such as NanoSIMS, with almost 100 nm lateral resolution [39] combining with depth profiling. Another equally interesting information is about the state of these copper contents. Thus far have we applied GIXRD and Raman on the copper treated bacteria (shown in SI, Figure 6), unfortunately no (or not enough) crystalline phase could be indexed.

With these observations, the role of bacteria in the antibacterial efficiency test (copper-PBS system) is summarised in Figure 7. The first phase is the release of copper ions when the contact of suspension and copper surface begins, which leads to an increase of copper content in suspension. The existence of bacteria does not essentially alter this initial phase. However, when these ions "meet" the bacteria, they begin to be accumulated by the bacteria, with two main paths confirmed: one is through the absorption of the bacteria. It is not the first time to report that the microbe may act as a reservoir of metal ions [40, 41], but to link this behaviour not only to the surrounding solution environment but also another object (in this case: copper surface) sharing the same environment is still seldom considered. Another path is the formation of copper phosphate sub-micron particles. As the bacteria begin to collect free copper ions from the solution, the amount of the actual copper ions in the solution has been gradually consumed. This process keeps the amount of free copper ion low, favouring less the oxide

formation. Exposure of copper surface without fully oxides coverage enables the continuous corrosion, explaining why the total amount of copper in the whole suspension is much higher.

At last, there are a few concerns that should be noticed basing on the current observations. For example, due to the additional effect introduced by bacteria, we should now realise the importance of interpreting the each corresponding scenario also with bacteria. In other words, although analysis of interaction between pure buffers and surface can help, but does not necessarily represent the actual situation (e.g. copper content level). On the other hand, the ion accumulation and its effects on corrosion process could be better validated, for instance, by well-defined experiments where copper content in the bacterial suspension can be precisely regulated. Moreover, further work should focus on the details of corrosion phenomenon on antibacterial copper as well as its consequences. Attempts to investigate how these changes could affect the antibacterial behaviour could also be meaningful.

4. Conclusions

This study focuses on copper surface evolution during the antibacterial efficiency test. The environmental components as well as the role of bacteria in buffer suspension were considered. Several concluding remarks are listed below:

- Copper surface oxidation in PBS is inhibited as the presence of *E. coli* in the suspension, confirmed by GIXRD and Raman. In contrast, without the Cu_2O coverage, localised corrosion attacks are much visible on the copper surface.
- Due to the absence of Cu_2O layer as an ion release barrier, the amount of copper ions released by the metallic surface strongly grows, where no plateau has been reached in 3 hours exposure.
- The released copper ions are found to be stored inside the bacteria and forming copper phosphate sub-micron particles outside the bacteria. These two main paths on one hand enhance the capacity of copper storage of the suspension, on the other hand, reduce the free copper ions in the suspension.
- This accumulation is a passive process where viable bacteria is not the necessary condition.

Acknowledgements

This study was supported by Erasmus Mundus Joint European Doctoral Programme in Advanced Materials Science and Engineering (DocMASE) and the Deutsch-Französische PhD-Track-Programme (PhD02-14). The ICP-MS experiments were supported by Dr. Ralf Kautenburger from the chair of Inorganic Solid State Chemistry. The authors acknowledge Prof. Volker Presser and Leibniz Institute for New Materials for the access of Raman spectrometer. Dr. Javad Najafi helped a lot to understand the concept of bacterial mobility. Prof. Gert-Wieland Kohring and Dr. Fabio Pereira from Department of Microbiology in Saarland University offer valuable instruction in centrifugation.

Declarations of interest

None.

Data availability

The data that support the findings of this study are available from the corresponding author on request.

References

[1] M. Vincent, R.E. Duval, P. Hartemann, M. Engels‐Deutsch, Contact killing and antimicrobial properties of copper, Journal of Applied Microbiology, 124 (2018) 1032-1046.

[2] R.J. Turner, Metal‐based antimicrobial strategies, Microbial Biotechnology, 10 (2017) 1062-1065.

[3] C. Rock, B.A. Small, K.A. Thom, Innovative Methods of Hospital Disinfection in Prevention of Healthcare-Associated Infections, Current Treatment Options in Infectious Diseases, 10 (2018) 65-77.

[4] M.P. Muller, C. MacDougall, M. Lim, I. Armstrong, A. Bialachowski, S. Callery, W. Ciccotelli, M. Cividino, J. Dennis, S. Hota, G. Garber, J. Johnstone, K. Katz, A. McGeer, V. Nankoosingh, C. Richard, M. Vearncombe, Antimicrobial surfaces to prevent healthcare-associated infections: a systematic review, Journal of Hospital Infection, 92 (2018) 7-13.

[5] M. Rosenberg, H. Vija, A. Kahru, C.W. Keevil, A. Ivask, Rapid in situ assessment of Cu-ion mediated effects and antibacterial efficacy of copper surfaces, Scientific Reports, 8 (2018) 8172.

[6] A. Rotini, A. Tornambè, R. Cossi, F. Iamunno, G. Benvenuto, M.T. Berducci, C. Maggi, M.C. Thaller, A.M. Cicero, L. Manfra, L. Migliore, Salinity-Based Toxicity of CuO Nanoparticles, CuO-Bulk and Cu Ion to Vibrio anguillarum, Frontiers in Microbiology, 8 (2017).

[7] H. Wu, X. Zhang, Z. Geng, Y. Yin, R. Hang, X. Huang, X. Yao, B. Tang, Preparation, antibacterial effects and corrosion resistant of porous Cu–TiO2 coatings, Applied Surface Science, 308 (2014) 43-49.

[8] M. Souli, A. Antoniadou, I. Katsarolis, I. Mavrou, E. Paramythiotou, E. Papadomichelakis, M. Drogari-Apiranthitou, T. Panagea, H. Giamarellou, G. Petrikkos, A. Armaganidis, Reduction of Environmental Contamination With Multidrug-Resistant Bacteria by Copper-Alloy Coating of Surfaces in a Highly Endemic Setting, Infection Control & Hospital Epidemiology, 38 (2017) 765-771.

[9] L.M. Gilbertson, E.M. Albalghiti, Z.S. Fishman, F. Perreault, C. Corredor, J.D. Posner, M. Elimelech, L.D. Pfefferle, J.B. Zimmerman, Shape-Dependent Surface Reactivity and Antimicrobial Activity of Nano-Cupric Oxide, Environmental Science & Technology, 50 (2016) 3975-3984.

[10] M. Ben-Sasson, X. Lu, S. Nejati, H. Jaramillo, M. Elimelech, In situ surface functionalization of reverse osmosis membranes with biocidal copper nanoparticles, Desalination, 388 (2016) 1-8.

[11] N.R. Dhineshbabu, V. Rajendran, Antibacterial activity of hybrid chitosan–cupric oxide nanoparticles on cotton fabric, Nanobiotechnology, IET, 10 (2016) 13-19.

[12] B. Demir, I. Cerkez, S.D. Worley, R.M. Broughton, T.-S. Huang, N-Halamine-Modified Antimicrobial Polypropylene Nonwoven Fabrics for Use against Airborne Bacteria, ACS Applied Materials & Interfaces, 7 (2015) 1752-1757.

[13] G. Irene, P. Georgios, C. Ioannis, T. Anastasios, P. Diamantis, C. Marianthi, W. Philippe, S. Maria, Copper-coated textiles: armor against MDR nosocomial pathogens, Diagnostic Microbiology and Infectious Disease, 85 (2016) 205-209.

[14] M. Turalija, P. Merschak, B. Redl, U. Griesser, H. Duelli, T. Bechtold, Copper(i)oxide microparticles - synthesis and

311 antimicrobial finishing of textiles, Journal of Materials Chemistry B, 3 (2015) 5886-5892.
312 [15] A. Usman, Z. Hussain, A. Riaz, A.N. Khan, Enhanced mechanical, thermal and antimicrobial properties of poly(vinyl
313 alcohol)/graphene oxide/starch/silver nanocomposites films, Carbohydrate Polymers, 153 (2016) 592-599.
314 [16] S. Kara, M.E. Ureyen, U.H. Erdogan, Structural and Antibacterial Properties of PP/CuO Composite Filaments Having Different
315 Cross Sectional Shapes, International Polymer Processing, 31 (2016) 398-409.
316 [17] A.P. Cano, A.V. Gillado, A.D. Montecillo, M.U. Herrera, Copper sulfate-embedded and copper oxide-embedded filter paper
317 and their antimicrobial properties, Materials Chemistry and Physics, 207 (2018) 147-153.
318 [18] S. Wu, S. Altenried, A. Zogg, F. Zuber, K. Maniura-Weber, Q. Ren, Role of the Surface Nanoscale Roughness of Stainless Steel
319 on Bacterial Adhesion and Microcolony Formation, ACS Omega, 3 (2018) 6456-6464.
320 [19] K. Ellinas, D. Kefallinou, K. Stamatakis, E. Gogolides, A. Tserepi, Is There a Threshold in the Antibacterial Action of
321 Superhydrophobic Surfaces?, ACS Applied Materials & Interfaces, 9 (2017) 39781-39789.
322 [20] C.E. Santo, E.W. Lam, C.G. Elowsky, D. Quaranta, D.W. Domaille, C.J. Chang, G. Grass, Bacterial Killing by Dry Metallic Copper
323 Surfaces, Applied and Environmental Microbiology, 77 (2011) 794-802.
324 [21] A. Tripathy, S. Sreedharan, C. Bhaskarla, S. Majumdar, S.K. Peneti, D. Nandi, P. Sen, Enhancing the Bactericidal Efficacy of
325 Nanostructured Multifunctional Surface Using an Ultrathin Metal Coating, Langmuir, 33 (2017) 12569-12579.
326 [22] J. Luo, C. Hein, F. Mücklich, M. Solioz, Killing of bacteria by copper, cadmium, and silver surfaces reveals relevant
327 physicochemical parameters, Biointerphases, 12 (2017) 020301.
328 [23] M. Hans, J.C. Támara, S. Mathews, B. Bax, A. Hegetschweiler, R. Kautenburger, M. Solioz, F. Mücklich, Laser cladding of
329 stainless steel with a copper–silver alloy to generate surfaces of high antimicrobial activity, Applied Surface Science, 320 (2014)
330 195-199.
331 [24] M. Hans, A. Erbe, S. Mathews, Y. Chen, M. Solioz, F. Mücklich, Role of Copper Oxides in Contact Killing of Bacteria, Langmuir,
332 29 (2013) 16160-16166.
333 [25] J. Zhao, D. Xu, M.B. Shahzad, Q. Kang, Y. Sun, Z. Sun, S. Zhang, L. Ren, C. Yang, K. Yang, Effect of surface passivation on
334 corrosion resistance and antibacterial properties of Cu-bearing 316L stainless steel, Applied Surface Science, 386 (2016) 371-380.
335 [26] H. Liu, D. Xu, K. Yang, H. Liu, Y.F. Cheng, Corrosion of antibacterial Cu-bearing 316L stainless steels in the presence of sulfate
336 reducing bacteria, Corrosion Science, (2017).
337 [27] C. Toparli, S.W. Hieke, A. Altin, O. Kasian, C. Scheu, A. Erbe, State of the Surface of Antibacterial Copper in Phosphate
338 Buffered Saline, Journal of The Electrochemical Society, 164 (2017) H734-H742.
339 [28] L.L. Foster, M. Hutchison, J.R. Scully, Corrosion of Cu-5Zn-5Al-1Sn (89% Cu, 5% Zn, 5% Al, 1% Sn) Compared to Copper in
340 Synthetic Perspiration During Cyclic Wetting and Drying: The Fate of Copper, Corrosion, 72 (2016) 1095-1106.
341 [29] K.P. Carter, A.M. Young, A.E. Palmer, Fluorescent Sensors for Measuring Metal Ions in Living Systems, Chemical Reviews, 114
342 (2014) 4564-4601.

[30] T.H. Hohle, W.L. Franck, G. Stacey, M.R. O'Brian, Bacterial outer membrane channel for divalent metal ion acquisition, Proceedings of the National Academy of Sciences of the United States of America, 108 (2011) 15390-15395.
[31] R.B.-K. Wakshlak, R. Pedahzur, D. Avnir, Antibacterial activity of silver-killed bacteria: the "zombies" effect, Scientific Reports, 5 (2015) 9555.
[32] C. Molteni, H.K. Abicht, M. Solioz, Killing of Bacteria by Copper Surfaces Involves Dissolved Copper, Applied and Environmental Microbiology, 76 (2010) 4099-4101.
[33] D.W. Hoeppner, Pitting corrosion: morphology and characterization, in: Framework, 1985, pp. 26.
[34] C. Hahn, M. Hans, C. Hein, R.L. Mancinelli, F. Mucklich, R. Wirth, P. Rettberg, C.E. Hellweg, R. Moeller, Pure and Oxidized Copper Materials as Potential Antimicrobial Surfaces for Spaceflight Activities, Astrobiology, (2017).
[35] U. von Stockar, J.S. Liu, Does microbial life always feed on negative entropy? Thermodynamic analysis of microbial growth, Biochimica et Biophysica Acta (BBA) - Bioenergetics, 1412 (1999) 191-211.
[36] C. Hahn, M. Hans, C. Hein, A. Dennstedt, F. Mücklich, P. Rettberg, C.E. Hellweg, L.I. Leichert, C. Rensing, R. Moeller, Antimicrobial properties of ternary eutectic aluminum alloys, BioMetals, (2018).
[37] G. He, W. Hu, C.M. Li, Spontaneous interfacial reaction between metallic copper and PBS to form cupric phosphate nanoflower and its enzyme hybrid with enhanced activity, Colloids and Surfaces B: Biointerfaces, 135 (2015) 613-618.
[38] Y.-K. Luo, F. Song, X.-L. Wang, Y.-Z. Wang, Pure copper phosphate nanostructures with controlled growth: a versatile support for enzyme immobilization, CrystEngComm, 19 (2017) 2996-3002.
[39] M.L. Kraft, P.K. Weber, M.L. Longo, I.D. Hutcheon, S.G. Boxer, Phase Separation of Lipid Membranes Analyzed with High-Resolution Secondary Ion Mass Spectrometry, Science, 313 (2006) 1948.
[40] F. Veglio, F. Beolchini, Removal of metals by biosorption: a review, Hydrometallurgy, 44 (1997) 301-316.
[41] J. Wang, C. Chen, Biosorbents for heavy metals removal and their future, Biotechnology Advances, 27 (2009) 195-226.

Figure Captions

Figure 1

Typical SEM images of copper surfaces after 3 hours of exposure to PBS **(a-b)** and PBS with *E. coli* **(c-d)**. The dashed squares in **(a)** and **(c)** indicate the positions of the following higher magnification images **(b)** and **(d)**. The arrows indicate localised corrosion attacks.

Figure 2

(a) High resolution grazing incidence X-ray diffractograms in the range of (111) planes of Cu_2O (#75-1531) and **(b)** typical Raman spectra obtained from copper surfaces after 3 hours exposure to PBS and PBS with *E. coli*. **(c)** OM images and SEM images of two typical features obtained from the bacterial treated surface and **(d)** their Raman spectra from the same areas.

Figure 3

Concentration of copper content in PBS, PBS with *E. coli* and its supernatant following various exposure periods. The error bars indicate the standard deviations calculated from three independent measurements.

Figure 4

Typical SEM images and EDS spectra from copper surface treated *E. coli* following various exposure periods, after being transferred to silicon wafer: **(a-c)** 1 hour; **(d-f)** 3 hours and **(g-i)** 6 hours. The dashed squares indicates the position of the following higher magnification images. The cross shape indicators point out the positions where the corresponding spectra were collected.

Figure 5

Typical SEM images **(a-b)** and EDS spectra **(c)** from 3 hours copper surface treated *E. coli*, on the original copper surface. The dashed squares indicates the position of the following higher magnification image. The cross shape indicators point out the positions where the corresponding spectra were collected.

Figure 6

Typical STEM observation from copper surface treated *E. coli* for 3 hours: **(a)** BF image; **(b)** ADF image. The dashed squares indicate the position of the following chemical mapping: **(c)** carbon; **(d)** oxygen; **(e)** phosphorus and **(f)** copper.

Figure 7

398 Schematic description of the main paths of copper ions in PBS in the presence of *E. coli*.

399

Table Captions

Table 1

The pH values of different solutions before and after 3 hours corrosion tests on copper surface.

Figure 1

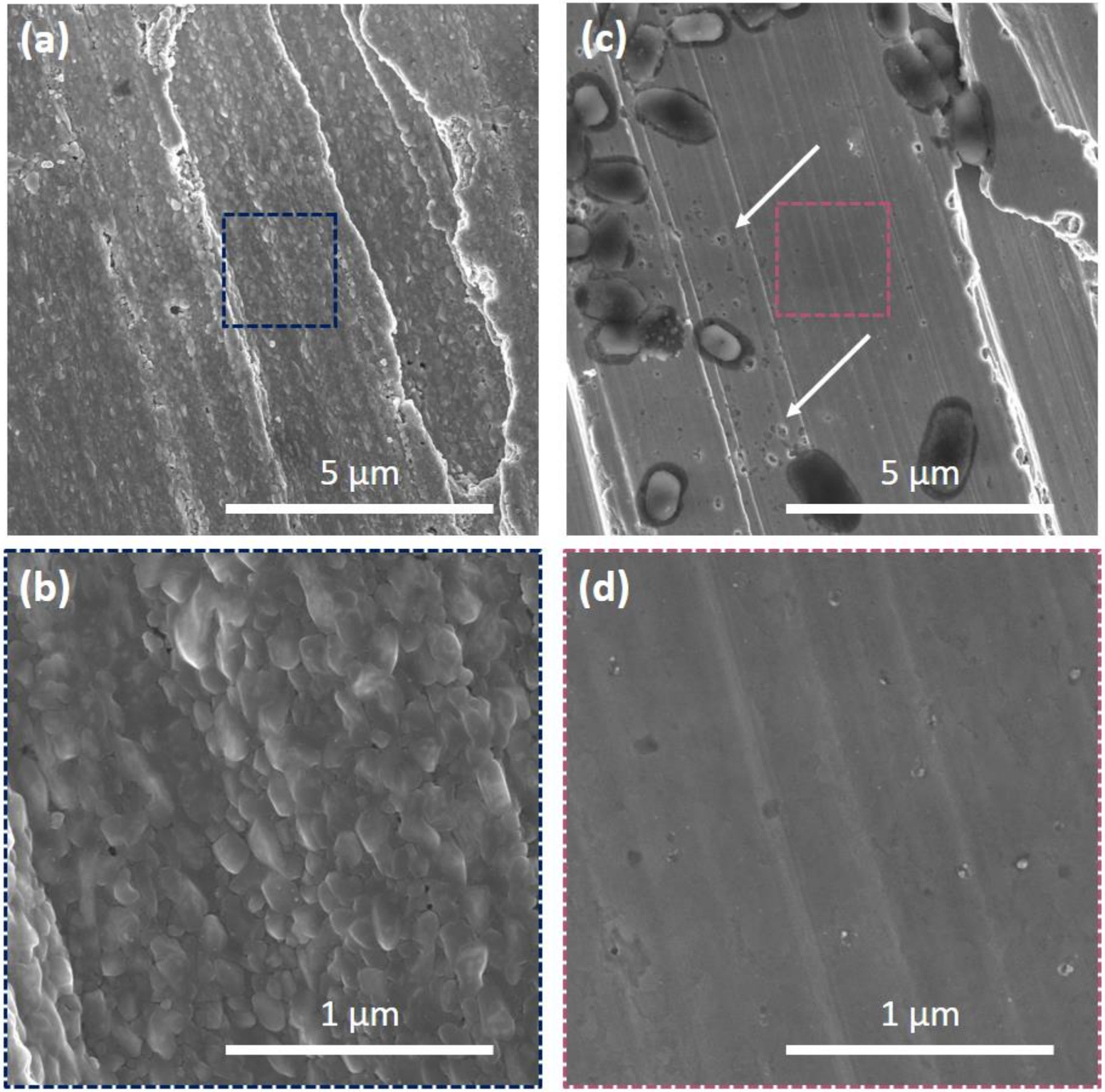

Figure 2

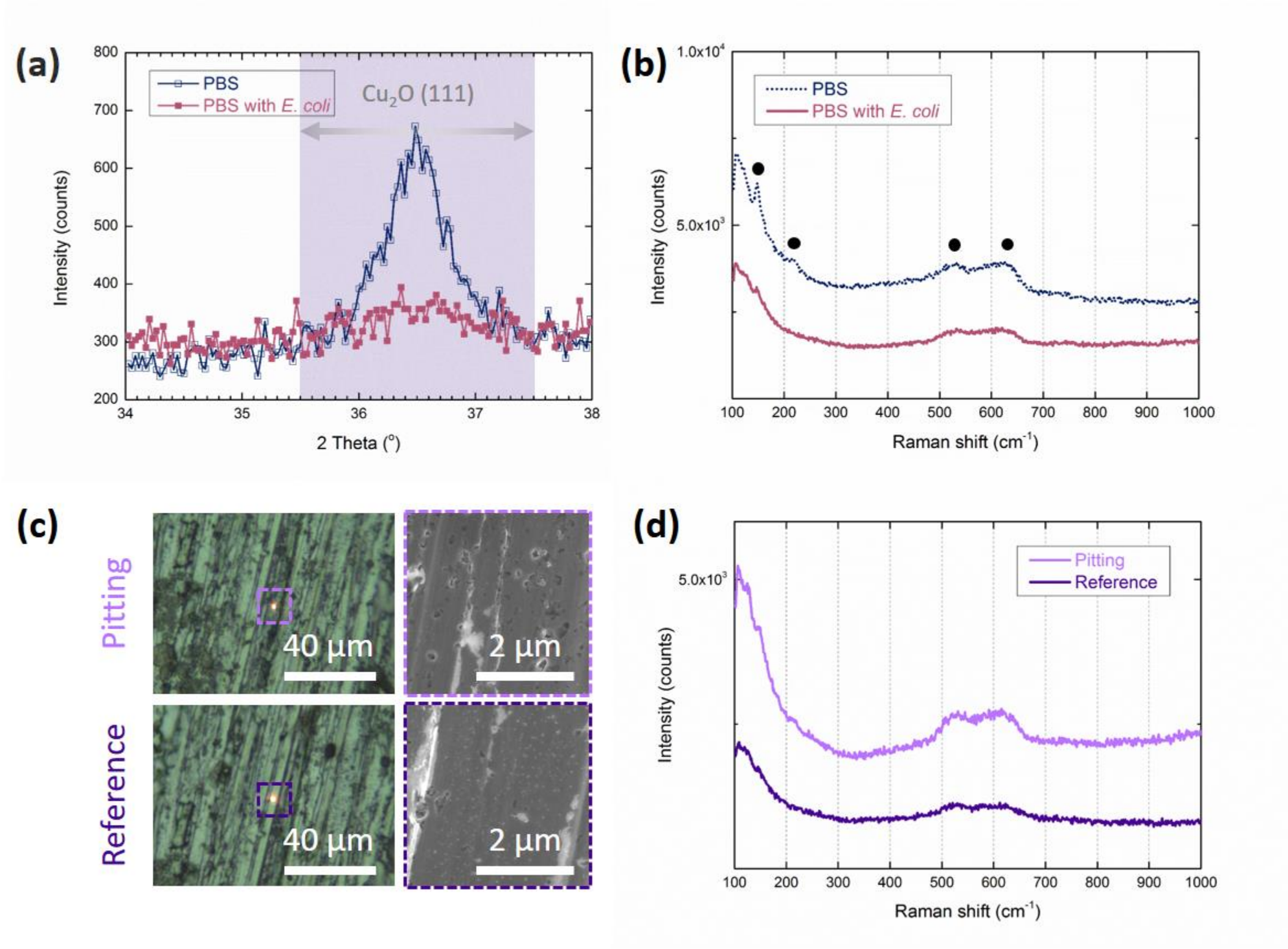
(a)
PBS
PBS with E. coli
Cu2O (111)
Intensity (counts)
2 Theta (°)
(b)
PBS
PBS with E. coli
Intensity (counts)
Raman shift (cm-1)
(c)
Pitting
Reference
40 μm
2 μm
40 μm
2 μm
(d)
Pitting
Reference
Intensity (counts)
Raman shift (cm-1)

Figure 3

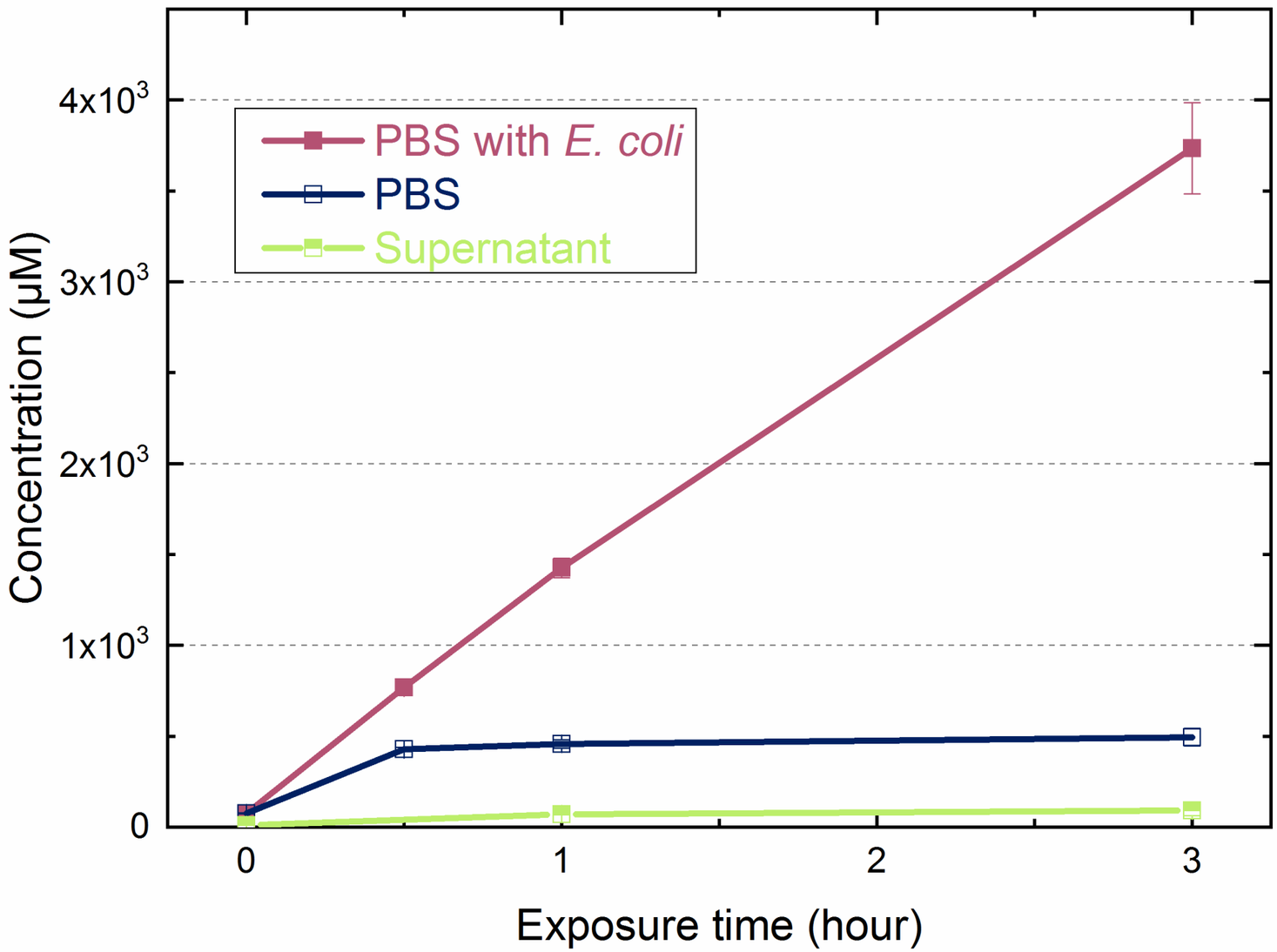
PBS with E. coli
PBS
Supernatant
Concentration (μM)
4x10^3
3x10^3
2x10^3
1x10^3
0
0
1
2
3
Exposure time (hour)

Figure 4

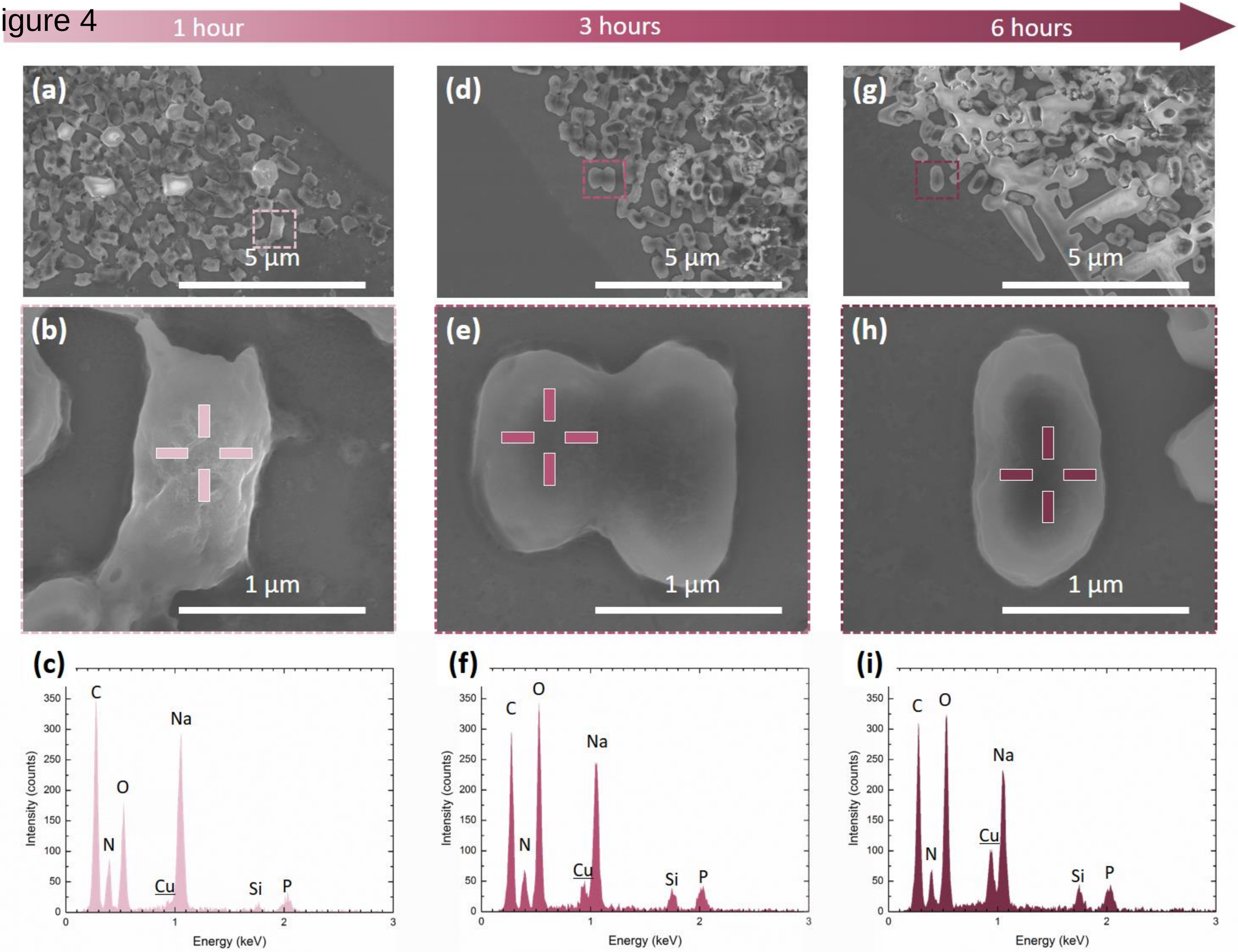
1 hour
3 hours
6 hours
(a)
5 µm
(d)
5 µm
(g)
5 µm
(b)
1 µm
(e)
1 µm
(h)
1 µm
(c)
C
O
N
Na
Cu
Si
P
Intensity (counts)
Energy (keV)
(f)
C
O
N
Na
Cu
Si
P
Intensity (counts)
Energy (keV)
(i)
C
O
N
Na
Cu
Si
P
Intensity (counts)
Energy (keV)

Figure 5

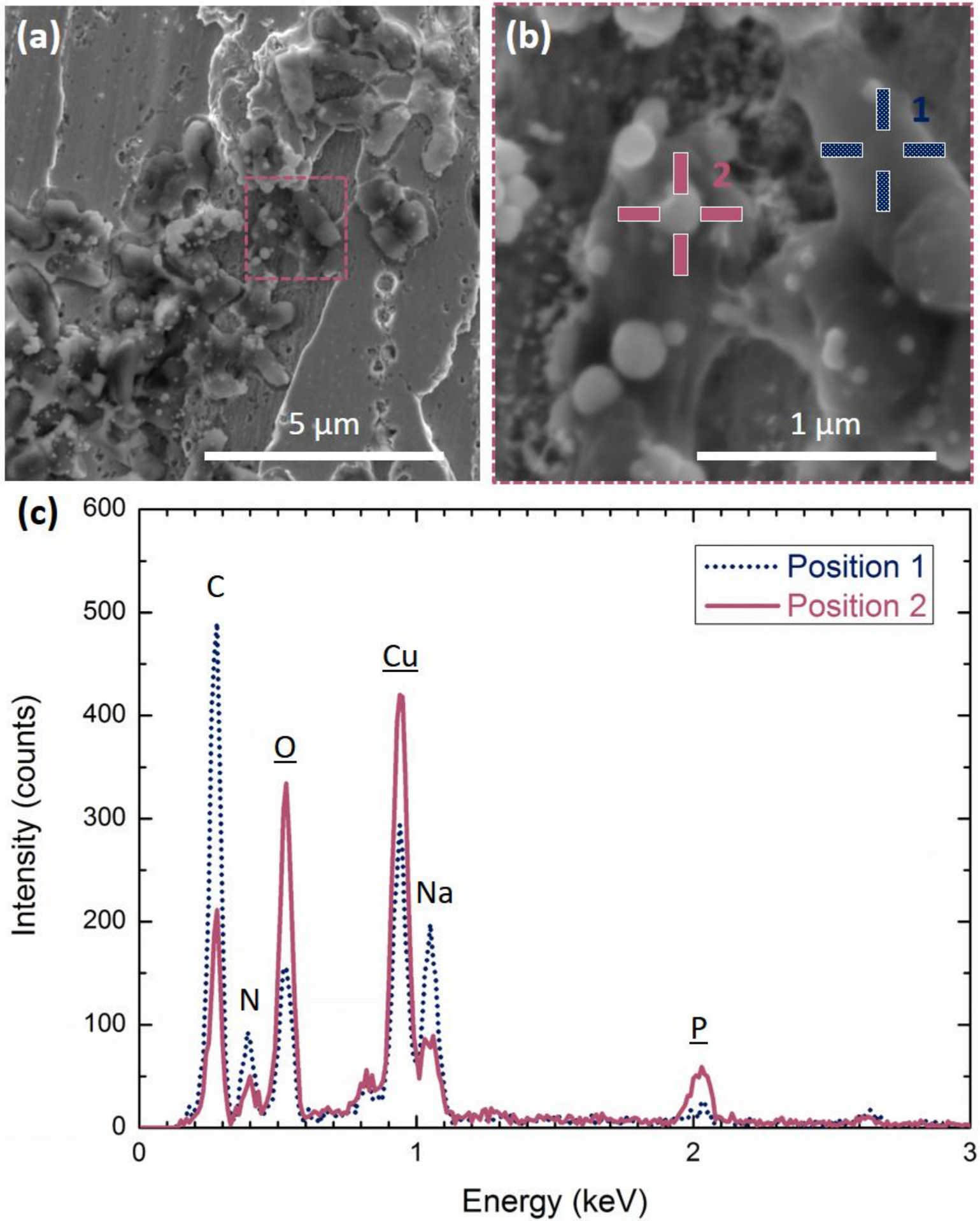
(a)
5 µm
(b)
1
2
1 µm
(c)
Position 1
Position 2
C
O
Cu
Na
N
P
Intensity (counts)
Energy (keV)
0
100
200
300
400
500
600
0
1
2
3

Figure 6

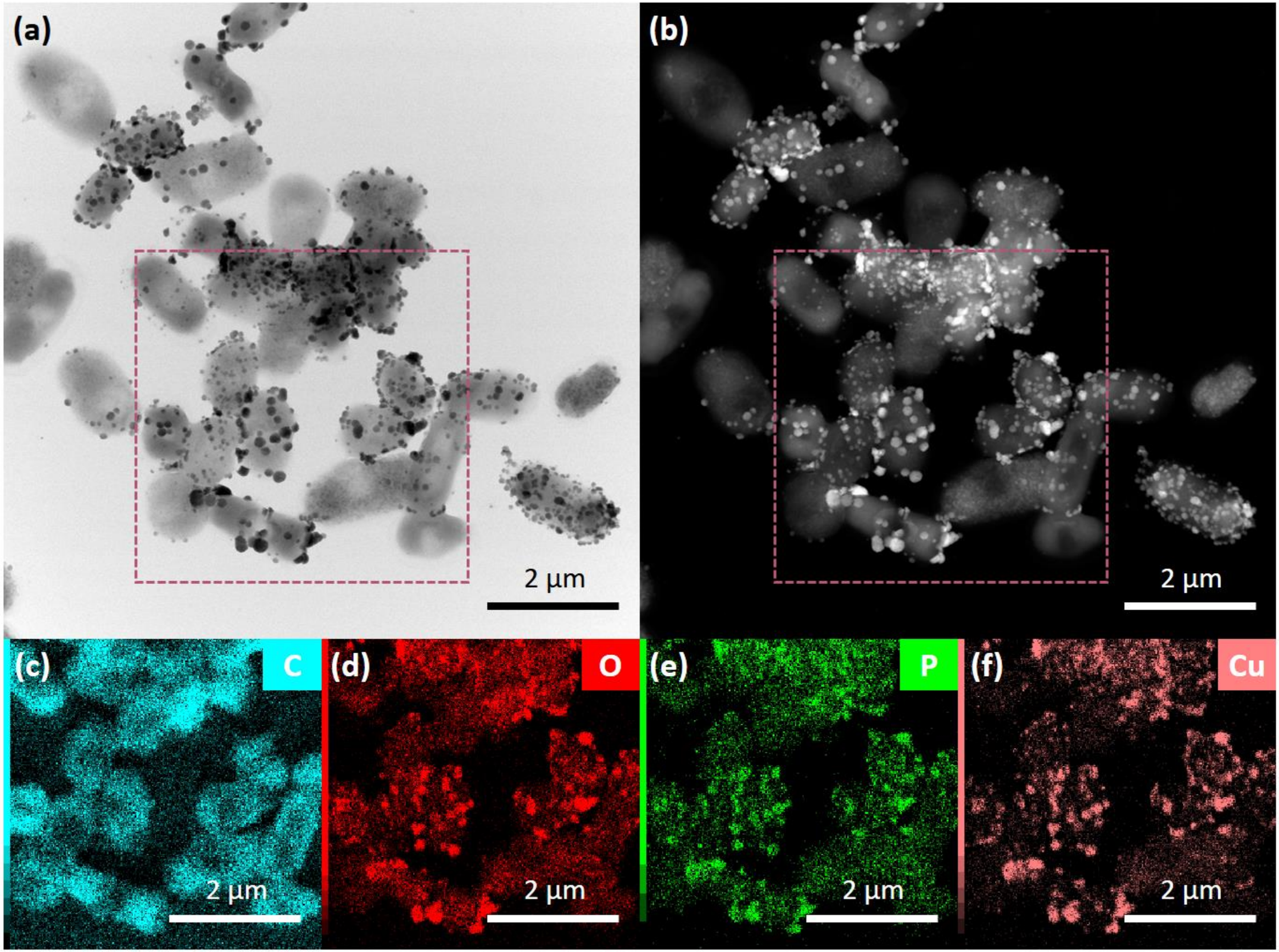

Figure 7

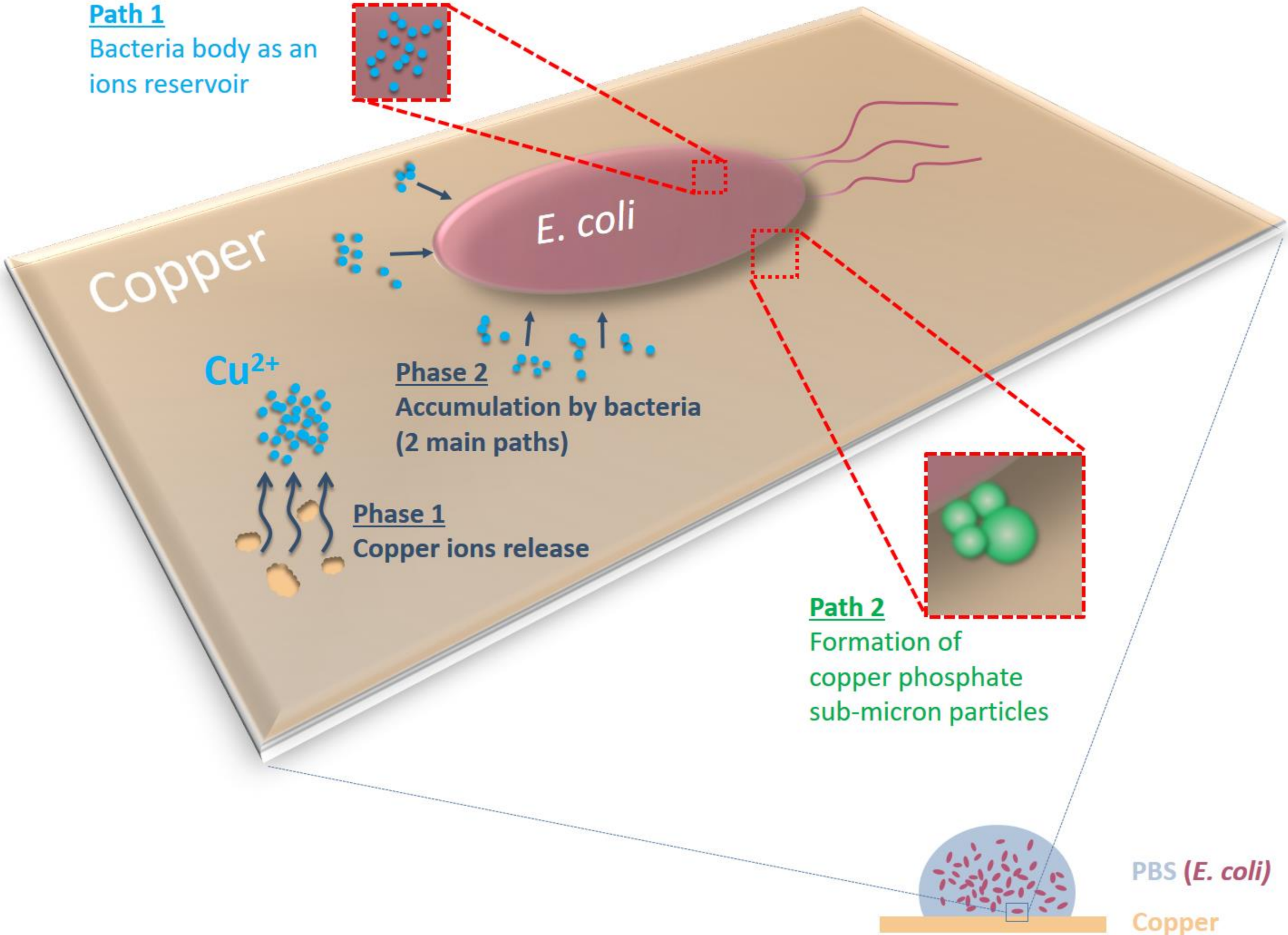
Path 1
Bacteria body as an ions reservoir
Copper
E. coli
Cu2+
Phase 2
Accumulation by bacteria (2 main paths)
Phase 1
Copper ions release
Path 2
Formation of copper phosphate sub-micron particles
PBS (E. coli)
Copper

Table 1

Solution	Before corrosion	After corrosion
PBS	7.4	7.7
PBS with *E. coli*	7.4	7.9
PBS with *S. cohnii*	7.4	7.9

Graphical Abstract

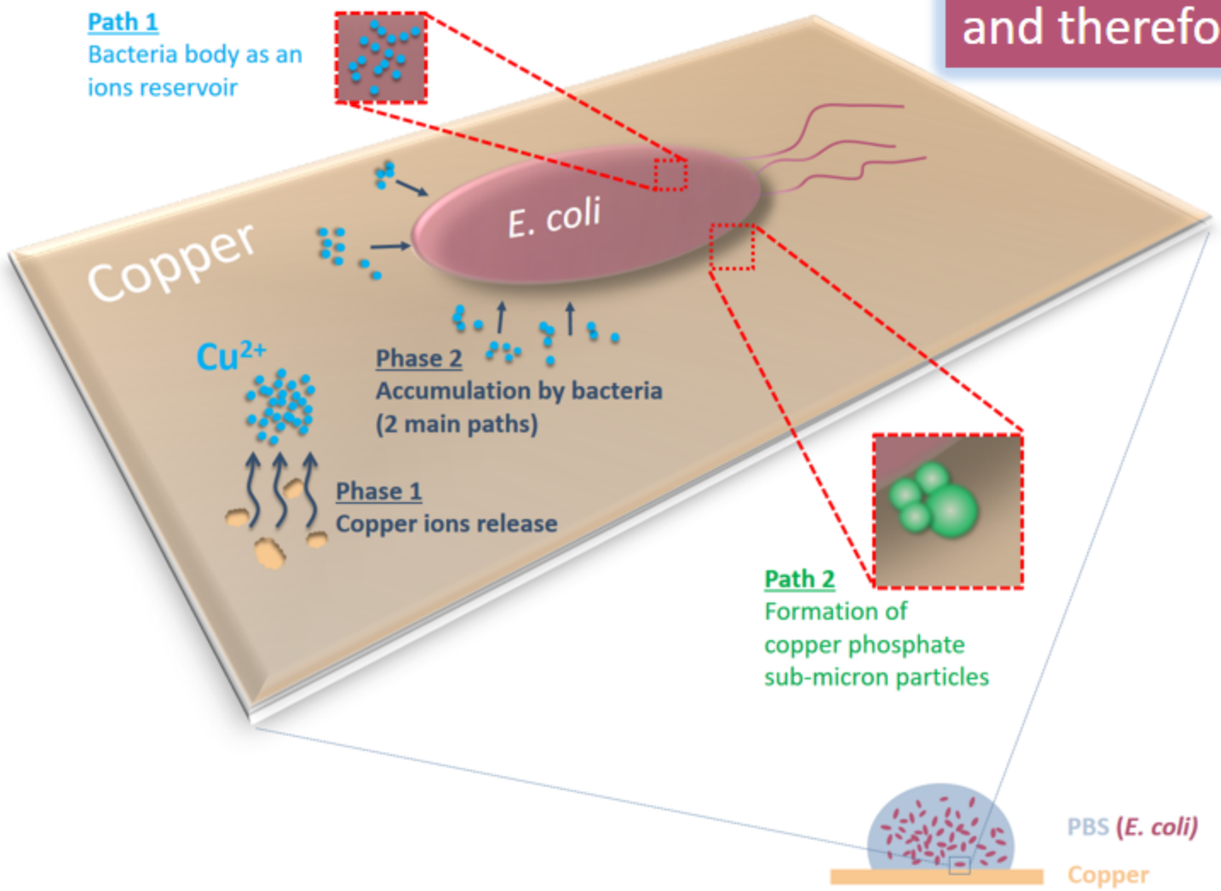

Accumulation of copper by bacteria inhibit the oxide formation and therefore dramatically promote the release of copper ions.